Palaeogeography, Palaeoclimatology, Palaeoecology 308 (2011) 1–11

Contents lists available at ScienceDirect

Palaeogeography, Palaeoclimatology, Palaeoecology

journal homepage: www.elsevier.com/locate/palaeo

# Terrestrial–marine teleconnections in the collapse and rebuilding of Early Triassic marine ecosystems

Thomas J. Algeo [a,*], Zhong Q. Chen [b], Margaret L. Fraiser [c], Richard J. Twitchett [d]

[a] Department of Geology, University of Cincinnati, Cincinnati, OH 45221, USA
[b] School of Earth and Environment, University of Western Australia, 25 Stirling Highway, Crawley, WA 6009, Australia
[c] Department of Geosciences, University of Wisconsin-Milwaukee, Milwaukee, WI 53211, USA
[d] School of Geography Earth & Environmental Sciences, University of Plymouth, Plymouth, PL4 8AA, UK

ARTICLE INFO

*Article history:*
Received 14 October 2010
Received in revised form 7 January 2011
Accepted 14 January 2011
Available online 21 January 2011

*Keywords:*
Permian–Triassic boundary
Mass extinction
Biotic crisis
Anoxia
Subaerial weathering
Eutrophication
Primary productivity

ABSTRACT

The latest Permian mass extinction (LPE), just prior to the Permian–Triassic boundary at ~252 Ma, resulted in the disappearance of ~90% of skeletonized marine taxa and the replacement of the Paleozoic Fauna by the Modern Fauna. In the immediate aftermath of the extinction, shallow-marine ecosystems were dominated by microbial communities and diminutive disaster taxa ("Lilliput faunas"), and the post-crisis period in general was characterized by high-abundance, low-diversity marine communities occupying a reduced ecological space. The recovery of marine ecosystems was a protracted process, lasting throughout the ~5-Myr-long Early Triassic. Some clades failed to recover and subsequently went extinct ("dead clades walking"), while others recovered only to suffer secondary crises during the Early Triassic. Profound environmental changes accompanied these biotic developments. Deep oceans experienced sustained hypoxia or anoxia for at least several million years following the boundary event. Anoxia was also widespread in shallow-marine areas, especially at the time of the LPE, but it was more episodic and abated more rapidly than in the deep ocean, making it an unlikely factor in the delayed recovery of Early Triassic marine ecosystems. The development of anoxia was due at least in part to a sharp temperature rise following the LPE but may have been stimulated by changes in marine nutrient inventories and productivity rates as well. These conditions may have been the result of a concurrent increase in subaerial weathering rates that was sustained into the Early Triassic. In addition to increasing nutrient fluxes to marine areas, rapid weathering caused a massive influx of sediment to shallow-marine systems, subjecting marine biotas to siltation stress. This scenario implies close teleconnections between terrestrial and marine environments during the Permian–Triassic boundary crisis, with perturbations of the terrestrial realm contributing to the marine crisis.



## 1. Introduction

This theme issue of *Palaeogeography Palaeoclimatology Palaeoecology* is devoted to studies of "Early Triassic Marine Ecosystems: Collapse and Rebuilding." The majority of papers included herein were presented at a session devoted to this topic at the North American Paleontological Congress (NAPC) held in Cincinnati, Ohio, on June 22–26, 2009. Both the present theme issue and the NAPC session are part of a larger research initiative focusing on Early Triassic ecosystems supported by International Geoscience Programme (IGCP) Project 572. This introductory article has two goals. First, it will summarize how each of the 18 papers comprising the present theme issue has advanced our understanding of the Permian–Triassic boundary (PTB) crisis and its aftermath. The contributions made by these studies will be presented in the context of a review of recent research on the effects of the LPE on marine biotas, the protracted recovery of marine ecosystems during the Early Triassic, and the environmental changes that caused and/or accompanied these developments. Second, this article will examine teleconnections between Permian–Triassic marine environments and the terrestrial realm. In particular, it will consider the role of terrestrial environmental changes in the collapse of latest Permian marine ecosystems, and the influence of terrestrial weathering rates and fluxes on the delayed recovery of Early Triassic marine ecosystems.

## 2. Collapse of marine ecosystems during the latest Permian crisis

The latest Permian extinction (LPE) at ~252 Ma was the largest biotic catastrophe of the Phanerozoic, resulting in the disappearance of ~90% of skeletonized marine species (Fig. 1; Alroy et al., 2008; Bambach et al., 2004; Erwin, 1994). Among the clades most strongly affected were radiolarians (Feng et al., 2007), foraminifera (Groves & Altinerer, 2005), corals (Flügel, 2002), brachiopods (Chen et al., 2005a,b), bryozoans (Powers & Pachut, 2008), echinoderms (Chen & McNamara, 2006; Twitchett & Oji, 2005), conodonts (Orchard, 2007; Stanley, 2009), and

* Corresponding author.
*E-mail address:* Thomas.Algeo@uc.edu (T.J. Algeo).

0031-0182/$ – see front matter © 2011 Elsevier B.V. All rights reserved.
doi:10.1016/j.palaeo.2011.01.011

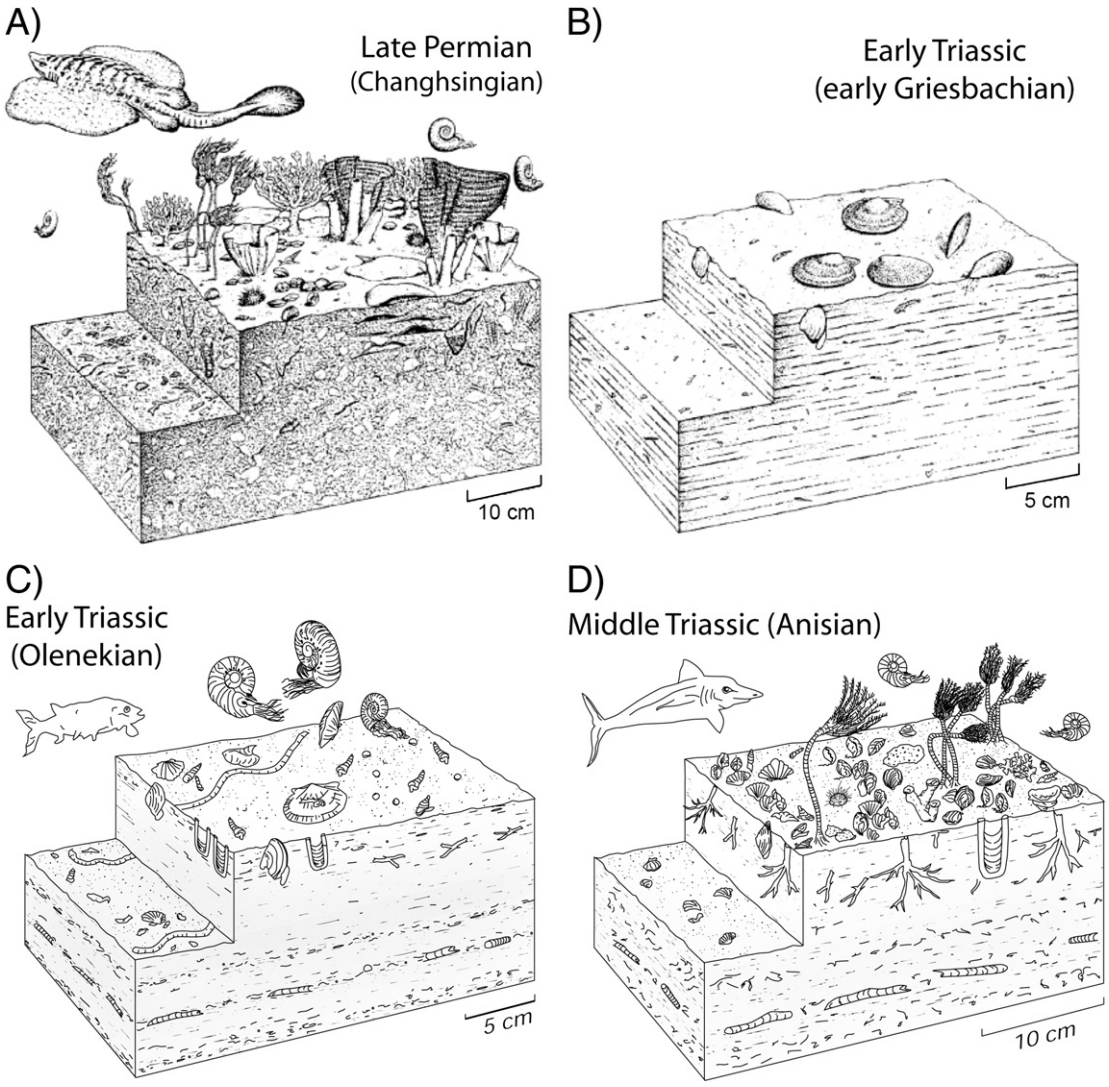


**Fig. 1.** Reconstructions of shallow-marine ecosystems in South China during the (A) Late Permian (pre-crisis), (B) Early Triassic (early Griesbachian, Induan), (C) Early Triassic (Olenekian), and (D) Middle Triassic (Anisian). The pre-crisis marine ecosystem (A) comprised a low-abundance, high-diversity community dominated by the Paleozoic Fauna (e.g., brachiopods, rugose corals, and crinoids). The early post-crisis ecosystem (B) comprised a high-abundance, low-diversity community dominated by opportunistic taxa of the Mesozoic Fauna (e.g., bivalves such as *Claraia*, ammonoids, and gastropods). Later ecosystems show evidence of substantial recovery, e.g., the rebound of a tracemaker community (C), and the reappearance of surviving members of the Paleozoic Fauna along with new elements of the Mesozoic Fauna in low-abundance, high-diversity communities (D). Panels A and B are from Benton and Twitchett (2003); panels C and D are original to this paper.

ammonoids (Brayard et al., 2006, 2009; McGowan, 2004; Stanley, 2009; Fig. 2). The disappearance of frame-building organisms resulted in a 'reef gap' that lasted through the Early Triassic (Fig. 3; Flügel, 2002; Pruss & Bottjer, 2005). The LPE also had a severe effect on terrestrial life (Benton, 2003; Grauvogel-Stamm & Ash, 2005; Krassilov & Karasev, 2009; Looy et al., 1999, 2001; Retallack, 1995; Wang, 1996). These developments coincided with a pronounced negative shift in the marine carbonate $\delta^{13}C$ record that marked the onset of a ~5-million-year-long interval of highly unstable conditions in the global carbon cycle (Figs. 2 and 3).

Brachiopods were one of the most diverse, abundant, and ecologically dominant clades of the Paleozoic but suffered a steep decline during the PTB crisis (Figs. 1 and 2; Chen et al., 2005a,b). Chen et al. (2011-this issue-a) document patterns of change in brachiopod diversity and ecology on the South China craton through the PTB interval. Brachiopods were highly abundant and diverse during the latest Permian (447 species in 143 genera) due to heightened ecological differentiation under stable environmental conditions but suffered high extinction rates during the LPE (92% of species and 86% of genera) as well as during a second extinction event in the earliest Triassic (84% of surviving species and 80% of surviving genera). Clues to the nature of the environmental disturbances that decimated brachiopods may be found in patterns of differential survival: shallow-marine forms, especially those living in reef communities, went extinct at high rates, whereas deep- and marginal-marine forms preferentially survived. In shallow-marine settings, spinal anchoring forms (which were adapted to muddy substrates; Leighton, 2000) went extinct at lower rates than other species. Burrowing forms also appear to have gone extinct at lower rates, although uncertainty exists owing to small numbers of taxa. The composition of benthic faunas is closely related to substrate character (Brett, 1998), and shifts among brachiopods toward spinose and burrowing forms are consistent with an increase in rapidly accumulating muddy sediments in Early Triassic shallow-marine environments (Algeo & Twitchett, 2010). Elevated sediment fluxes would have disproportionately harmed species that required stable environmental conditions and that were not well adapted to soft, unstable substrates.

In the immediate aftermath of the LPE, microbialites flourished on many shallow tropical shelves and platforms, especially within the Tethyan region (Fig. 3; Baud et al., 1997, 2007; Kershaw et al., 1999;

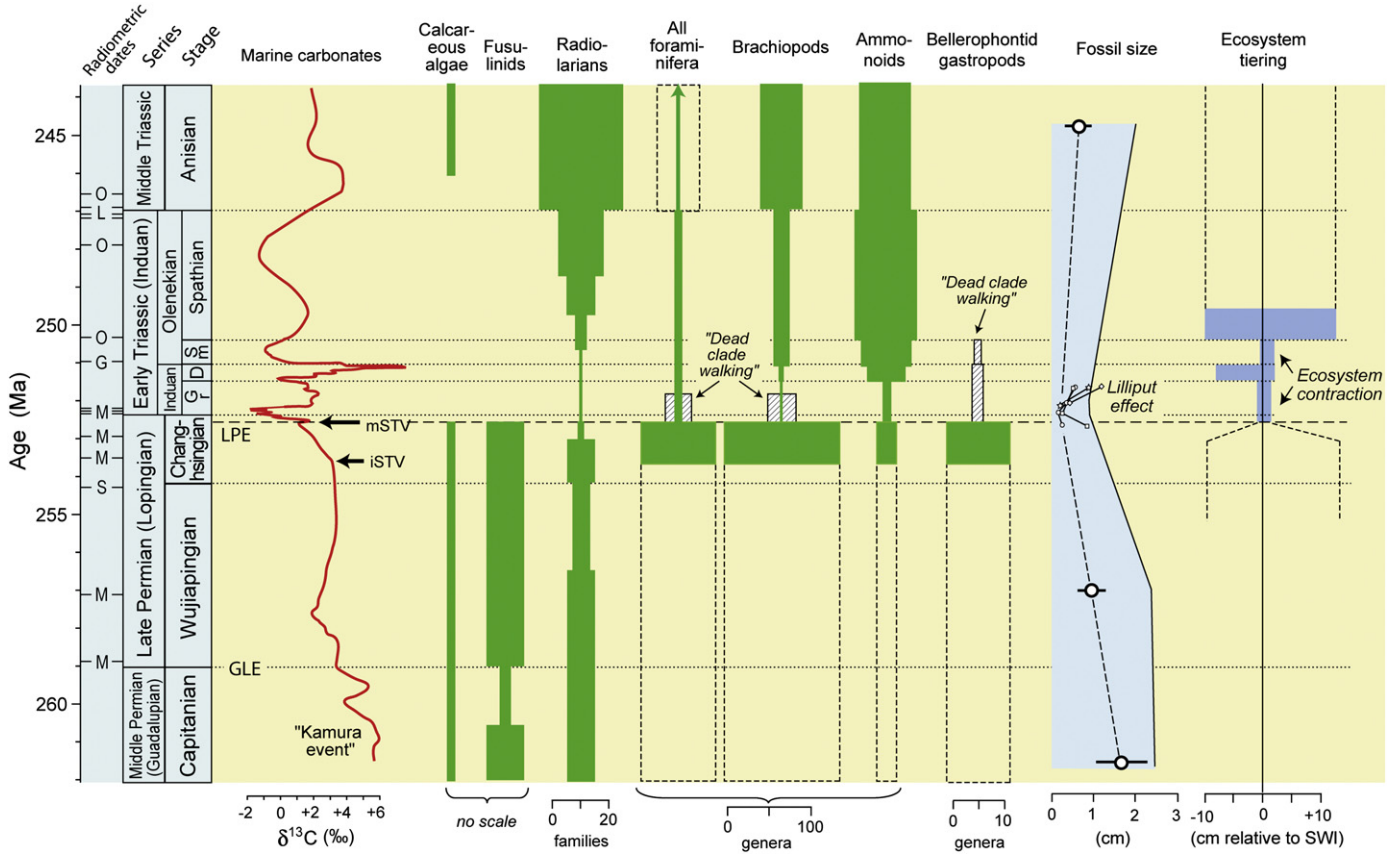


**Fig. 2.** Biodiversity and ecological patterns during the Middle Permian to Middle Triassic. Carbon isotope data from Isozaki et al. (2007b), Korte and Kozur (2010), Korte et al. (2005a,b), and Payne et al. (2004). Biodiversity data: calcareous algae (Pruss & Bottjer, 2005), radiolarians and fusulinids (Isozaki, 2009; Racki & Cordey, 2000), foraminifera (Groves & Altiner, 2005), brachiopods (Chen et al., 2005a), ammonoids (Brayard et al., 2006; McGowan, 2004, 2005), and bellerophontid gastropods (Kaim & Nützel, 2011-this issue). Note that redating of the Qudenggongba Formation of the Tulong Group to the Anisian–Ladinian indicates that bellerophontids survived until the Middle Triassic (M. Clapham, pers. comm. 2010) rather than to the Smithian–Spathian boundary as reported by Kaim and Nützel (2011-this issue). Ecosystem tiering data are from Twitchett (1999) and fossil size data from Twitchett (2007); open circles represent gastropods, small symbols (confined to latest Changhsingian and Griesbachian) represent specific genera: squares = *Bellerophon*, circles = *Lingula*, diamonds = *Claraia*, and stars = *Unionites*. Time scale based on radiometric dates from: M = Mundil et al. (2004), L = Lehrmann et al. (2006), O = Ovtcharova et al. (2006), G = Galfetti et al. (2007), and S = Shen et al. (2010). Note that the Griesbachian (Gr), Dienerian (D), Smithian (Sm), and Spathian are substages of the Early Triassic. GLE = Guadalupian–Lopingian event, LPE = latest Permian event, iSTV and mSTV = initial and main-stage Siberian Traps volcanism (based on Kozur & Weems, 2011-this issue), and SWI = sediment–water interface.

Lehrmann, 1999; Schubert & Bottjer, 1992; Weidlich & Bernecker, this issue). Their period of widespread growth was short, only from the *N. meishanensis* Zone to the *I. staeschei* Zone at Meishan D (Yang et al., 2011-this issue), or an interval of ~150 kyr (S. Bowring, unpubl.; Chen et al., 2009), although microbialites reappeared at least three more times during the Early Triassic (Fig. 3; Baud et al., 2007; Pruss & Bottjer, 2005). The significance of this 'anachronistic facies' (Baud et al., 2007) is unclear: did microbial mats thrive because environmental conditions remained hostile to metazoans during this interval, or, alternatively, because the metazoan biota was so completely decimated during the extinction event (Fig. 2) that the surviving populations were inadequate to the task of rapidly recolonizing many shallow-marine habitats? (cf. Schubert & Bottjer, 1992). Intriguingly, the stratigraphic distribution of microbialites appears to be related to maxima of marine carbonate $\delta^{13}C$ (except at the LPE) and conodont and ammonoid diversity, as well as to possible peaks in chemical weathering rates (Fig. 3; Algeo & Twitchett, 2010; Algeo, unpubl. data). These relationships may record the influence of weathering rates on marine primary productivity, food resource availability at higher trophic levels, and eutrophic conditions favoring microbial mats over benthic algae, corals, and other comparatively slow-growing metazoans (Fig. 2).

Detailed studies of PTB microbialites are required in order to gain insights into the issues discussed above. Yang et al. (2011-this issue) examine the composition of microbialite communities in sections from South China, which show three different growth forms. Thrombolites are dominated by *Renalcis* and foraminifers but also contain ostracods, microgastropods, and microconchids. Stromatolites are dominated by coccoidal microbes with minor constituents of other undetermined microbes. Dendrolites contain few identifiable microfossils; metazoans are rare in all three communities. Chen et al. (2011-this issue-b) study the molecular records of South China microbialites. The LPE horizon is marked by changes in the ratios of pristane/phytane and $C_{17}/C_{18}$ *n*-alkanes indicative of a transient suppression of autotroph productivity, and by changes in the ratio of branched to normal $C_{17}$ alkanes indicative of enhanced inputs from heterotrophs. Dominance of low-molecular-weight *n*-alkanes suggests that algae and bacteria were the dominant contributors to the organic fraction, with bacteria particularly enhanced within the stromatolite facies relative to other lithofacies (including both skeletal limestones and thrombolitic microbialites).

## 3. Recovery of marine ecosystems during the Early Triassic

The pattern of recovery of marine ecosystems during the Early Triassic is of particular interest owing to the fact that it marks the replacement of the Paleozoic Fauna by the Modern Fauna (Fig. 1; Sepkoski, 1982, 2002). Diversity within individual clades as well as marine ecosystems as a whole shows broadly similar patterns (Figs. 2 and 3): a rapid decline during the LPE, a minimum during the Griesbachian Substage (early Induan Stage), a degree of recovery ranging from weak to strong (depending on clade) during the Dienerian

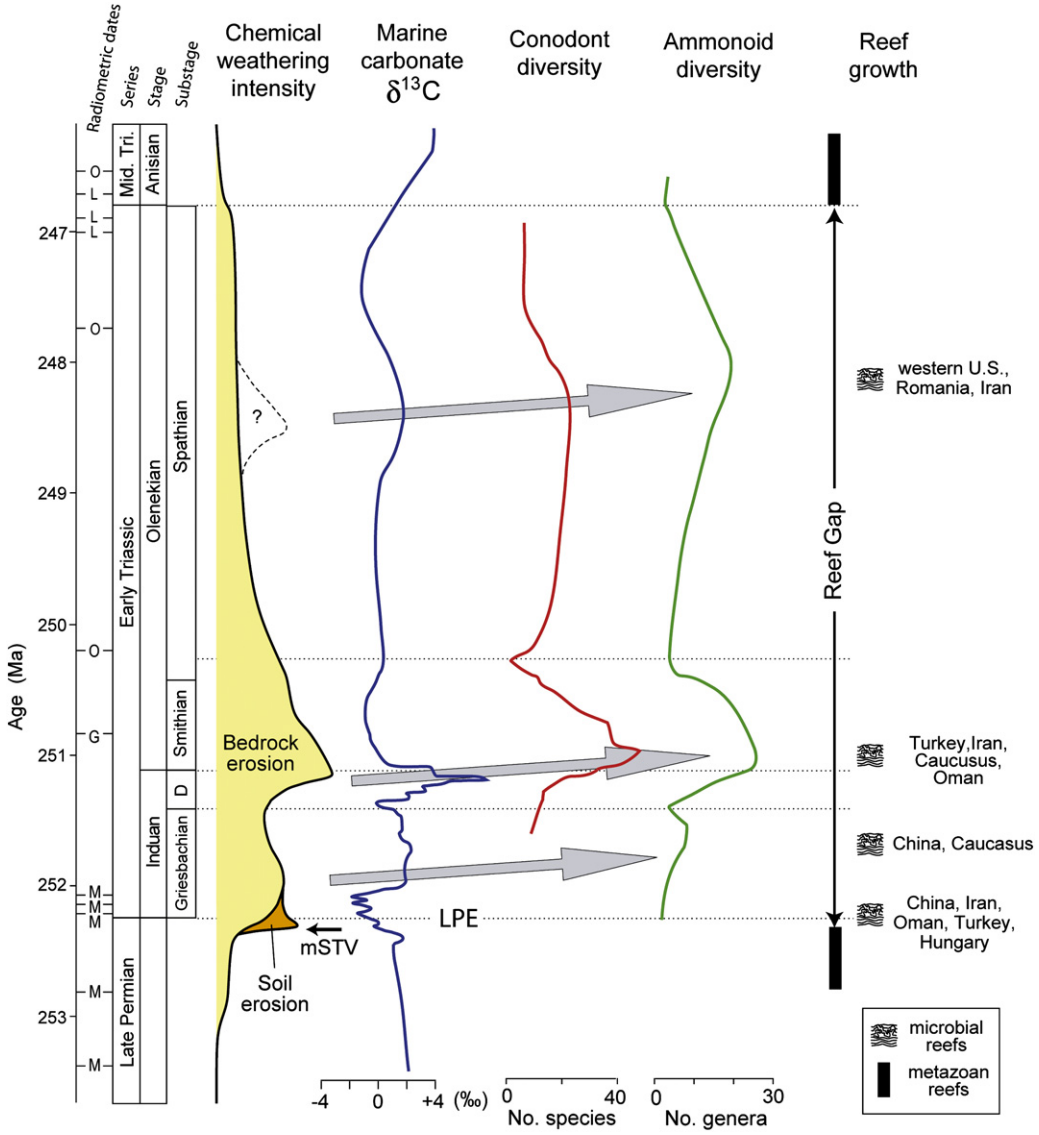


**Fig. 3.** High-resolution profiles for Late Permian–Early Triassic. Chemical weathering intensity based on Algeo and Twitchett (2010) and Algeo (unpubl. data); orange and yellow fields represent soil and bedrock erosion, respectively. Conodont and ammonoid diversity data from Stanley (2009); microbial reef data from Baud et al. (2007), Lehrmann (1999), Pruss and Bottjer (2004), Weidlich and Bernecker (this issue), and Woods et al. (1999). Other sources and abbreviations as in Fig. 2. Arrows indicate related peaks in the profiles shown.

(late Induan) and Smithian (early Olenekian Stage) substages, followed by a robust recovery during the Spathian Substage (late Olenekian) and into the Middle Triassic (e.g., Payne et al., 2004, 2006). Forel et al. (2011-this issue) show that ostracods followed this diversity pattern during the Early Triassic. Ostracod lineages that survived the crisis were dominated by burrowing and deposit-feeding forms, especially those from the distal shelf environment (such as the smooth-shelled Bairdiidae). Fraiser (2011-this issue) examines secular changes in skeletobionts, i.e., encrusting organisms such as microconchids. Although generally impoverished relative to skeletobiont assemblages of other ages, Early Triassic assemblages show increases in diversity, abundance, and tiering during recovery of marine ecosystems from the PTB crisis.

Recovery rates following the LPE varied among marine invertebrate clades. For example, ammonoid faunas recovered relatively rapidly, reaching a level of diversity by the early Olenekian that exceeded that of the Late Permian (Figs. 2 and 3; Brayard et al., 2006, 2009; Stanley, 2009; Zakharov & Popov, this issue). Conodonts also showed a relatively rapid recovery with a major diversification event during the Dienerian, followed by repeated further episodes of extinction and reradiation (Ji et al., 2011-this issue; Orchard, 2007; Stanley, 2009). Both groups show a major decline around the Smithian–Spathian boundary, synchronous with a large (+4 to +8‰) shift in C-isotopic compositions (Fig. 3; Payne et al., 2004; Tong et al., 2007a) reflecting a major increase in organic carbon burial rates possibly related to elevated marine productivity. The rapid recovery of ammonoids and conodonts during the Early Triassic, as well as their vulnerability to episodic post-LPE environmental disturbances, may have been related to their position in the marine trophic web. Changes in the composition or productivity of phytoplankton communities during the Early Triassic (Algeo et al., in review; Knoll et al., 2007; Payne & van de Schootbrugge, 2007) are likely to have had different consequences for nektic versus benthic organisms. Such changes may have produced a highly varied range of trophic resources or food chains ("poikilotrophism") for nekton that encouraged rapid evolutionary diversification, whereas the sinking flux of organic matter available to benthic communities showed comparatively little change in character.

Not all lineages that survived the LPE prospered in the aftermath of the crisis. Early Triassic ecosystems contain various taxa belonging to biotic groups that survived but failed to rediversify and that subsequently went extinct by the Middle Triassic. These groups have been

termed "dead clades walking" (in reference to the film Dead Man Walking; Jablonski, 2001, 2002). Surviving elements of the Paleozoic Fauna were particularly prone to this phenomenon. For example, brachiopods suffered high rates of extinction at the LPE (98% at the generic level), and a large majority of the surviving genera (~90%) subsequently went extinct during the Early Triassic, including all productids (Fig. 2; Chen et al., 2005b, 2006, 2009; Chen, 2011-this issue-a). Among the surviving brachiopod lineages, a few thrived and evolved into new "Mesozoic-type" clades, as documented in a study of Lower Triassic marine faunas from eastern Russia (Zakharov & Popov, this issue). Other examples of "dead clades walking" are present among the foraminifera, with ~20 genera that survived the LPE going extinct during the Early Triassic (Song et al., 2009), and the bellerophontid family of gastropods, with 8 species belonging to three genera that survived the LPE going extinct during the Early to Middle Triassic (Fig. 2; Kaim & Nützel, 2011-this issue). Among the bellerophontids, some taxa continued to have a global distribution with locally high abundances during much of the Early Triassic, making the reasons for their subsequent disappearance enigmatic. In general, the reasons why certain lineages that survive a mass extinction event fail to rediversify when other lineages do so vigorously are poorly understood but might be sought in the dynamics of marine ecosystem redevelopment and reintegration, i.e., in the new patterns of interspecific relationships that evolve as more complex trophic systems are reestablished.

Early Triassic marine assemblages commonly exhibit a sharp reduction in the size of body fossils, i.e., the "Lilliput effect," among both surviving and newly evolved taxa in the aftermath of the mass extinction event (Figs. 1 and 2; Fraiser & Bottjer, 2004; Payne, 2005; Twitchett, 1999, 2007). Some species exhibit a rapid recovery of body size during the earliest Triassic (Griesbachian), although most lineages continued to increase in body size throughout the Early Triassic. The ecological significance of reduced body size is uncertain but may be linked to more rapid generational turnover, an adaptive response of populations living in stressed or episodically disturbed environments. In a study of miniaturization among Early Triassic foraminifera, Song et al. (2011-this issue) demonstrate that protozoans exhibited the Lilliput effect due to a combination of preferential extinction of large forms, reduced size of surviving forms, and evolution of small forms following the crisis. Metcalfe et al. (2011-this issue) evaluate whether miniaturization was a consequence of reduced growth rates or shorter life cycles by analyzing growth banding in Early Triassic bivalves (*Unionites*, *Claraia*), gastropods (*Bellerophon*), and brachiopods (*Lingula*). More closely spaced growth lines provide evidence of slower growth that may be an indication of the persistence of suboptimal environmental conditions in shallow-marine settings during the Early Triassic.

The composition and structure of marine communities underwent profound changes in the aftermath of the LPE. In addition to smaller body sizes, marine assemblages are characterized by high abundance, low diversity, and a proliferation of small, infaunal deposit feeders (Fig. 1; Chen et al., 2010; Twitchett, 1999, 2007). Although taxonomic dominance in marine communities shifted from the Paleozoic Fauna to the Modern Fauna at the PTB, the shift in "ecological dominance" (Clapham et al., 2006) between these faunas did not necessarily occur simultaneously. In a survey of bioclastic deposits of Middle Triassic age, Greene et al. (2011-this issue) show that ecological dominance varied globally, with Paleozoic faunal elements such as brachiopods and crinoids dominant at some localities and Modern faunal elements such as bivalves dominant at others. However, Jacobsen et al. (2011-this issue) offer a cautionary note regarding methodological procedures for evaluating ecological dominance in paleomarine communities, as different methods can yield different results.

The rate of recovery of marine ecosystems varied regionally. Areas of relatively rapid recovery included some tropical Tethyan carbonate platforms (Krystyn et al., 2003; Twitchett et al., 2004), boreal shallow-marine shelves (Beatty et al., 2008), and some deep-shelf systems along the western Pangaean margin (Rodland & Bottjer, 2001). Jacobsen et al. (2011-this issue) report on differences in recovery patterns between marine communities occupying similar paleoclimatic and paleogeographic settings: Early Triassic assemblages from Oman exhibit markedly higher diversity and greater evenness of species abundances than assemblages from similar carbonate platform facies in northern Italy. Regional variation is also evident in clade-specific patterns of post-crisis diversification. For example, ammonoids rediversified in both tropical and boreal regions following the LPE, but brachiopods showed almost no recovery in boreal regions (Zakharov & Popov, this issue).

## 4. Terrestrial influences on the collapse and recovery of Permian–Triassic marine ecosystems

Long-term tectonic and climatic changes were underway during the Middle and Late Permian that may have created conditions conducive to the PTB crisis. The formation of the Pangean supercontinent generated large arid to semi-arid regions in continental interiors that expanded as monsoonal circulation weakened (Parrish, 1993). The Tethys Ocean became an equatorial cul-de-sac that served as a nutrient trap, resulting in generally high levels of primary productivity and benthic oxygen demand (Winguth & Maier-Reimer, 2005). Changes in marine ecosystems began as early as the Guadalupian (late Middle Permian), as evidenced by extinctions among radiolarians, fusulinacean foraminifera, and calcareous algae (Isozaki, 2009; Isozaki et al., 2007a; Wignall et al., 2009). At that time, molluscs expanded into deeper shelf and slope habitats that were simultaneously vacated by brachiopods and bryozoans (Bottjer et al., 2008; Clapham & Bottjer, 2007; Powers & Pachut, 2008). These trends coincided with an interval of intensified upwelling, marine productivity, and organic carbon burial that resulted in a climatic cooling episode known as the "Kamura event" (Fig. 2). The Kamura event was first recognized from the western Pangean margin (Beauchamp & Baud, 2002) and from Panthalassic Ocean atolls (Isozaki, 2009; Isozaki et al., 2007a), but Isozaki et al. (2011-this issue) demonstrate its global character by identifying its characteristic $^{13}C$-enriched carbon-isotopic signature in a western Tethyan succession from Slovenia. The LPE itself was preceded by a second-order extinction event at the Middle–Late Permian boundary (the Guadalupian–Lopingian event; Fig. 2; Stanley & Yang, 1994) that has been linked to the eruption of a mantle plume (the Emeishan Large Igneous Province) in southwestern China (Zhou et al., 2002).

The ultimate cause(s) of the LPE remain under debate. As a meteorite impact mechanism (Becker et al., 2001, 2004; Kaiho et al., 2001) has been largely discredited (Farley et al., 2005; Müller et al., 2005), the leading hypothesis at present is the eruption of the Siberian Traps (Fig. 5). This massive outpouring of flood basalts has been dated to ~252–250 Ma (Campbell et al., 1992; Reichow et al., 2009; Renne et al., 1995), making its age indistinguishable from that of the PTB within the limits of radiometric age uncertainties (see review in Mundil et al., 2010). In order to better define the relationship between Siberian Traps volcanism and coeval marine events, Kozur and Weems (2011-this issue) attempt to correlate terrestrial successions in the Germanic Basin and Siberia with the PTB stratotype section at Meishan, China. Their study infers that the onset of explosive silicic volcanism in the Siberia Traps volcanic system dates to the early Changhsingian *Clarkina bachmanni* Zone, which also marks the onset of a protracted negative shift in carbonate C-isotopes during the Late Permian (Fig. 2; Korte & Kozur, 2010). They also infer that the onset of major flood basalt volcanism in Siberia coincided with the latest Changhsingian *Clarkina meishanensis–Hindeodus praeparvus* Zone (= bed 24e of Meishan D; Zhang et al., 2007), correlative with the lower *Falsisca postera* zone of the Germanic Basin and with marine interbeds in Siberia containing *Falsisca turaika–F. podrabineki*, as well as with the widely identified 3 to 4‰ negative shift in C-isotopic records coincident with the LPE horizon (Fig. 2; Korte & Kozur, 2010). These findings support a link between volcanic activity in Siberia and

contemporaneous changes in marine ecosystems and the global carbon cycle.

Although the environmental changes initiated by the eruption of the Siberian Traps were profound (Figs. 4 and 5), the exact nature of those changes and their effects on marine ecosystems are not well understood (cf. Benton & Twitchett, 2003). Release of a combination of volcanic $CO_2$ and thermogenic methane produced when magmas intruded into West Siberian coal basins is thought to have triggered strong climatic

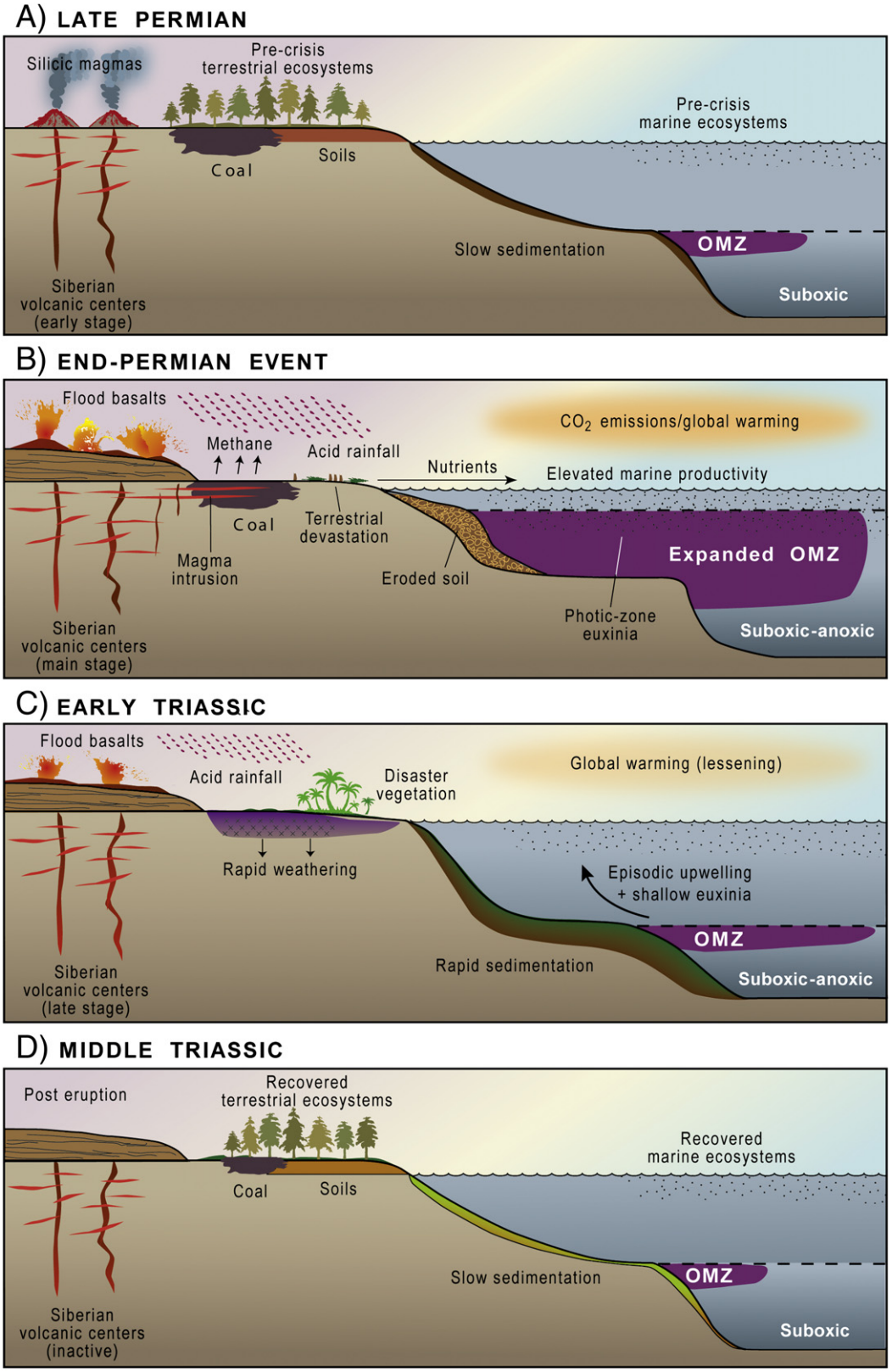


**Fig. 4.** Interpretative reconstructions of terrestrial–marine teleconnections during the PTB crisis. Early stage Siberian Traps volcanism with minimal environmental effects during the Late Permian (A). Main stage eruptions with attendant environmental effects during the latest Permian (B). Late stage eruptions with lessening environmental effects during the first part (Induan Stage) of the Early Triassic (C). Post-eruption recovery of terrestrial and marine ecosystems by the Middle Triassic (D).

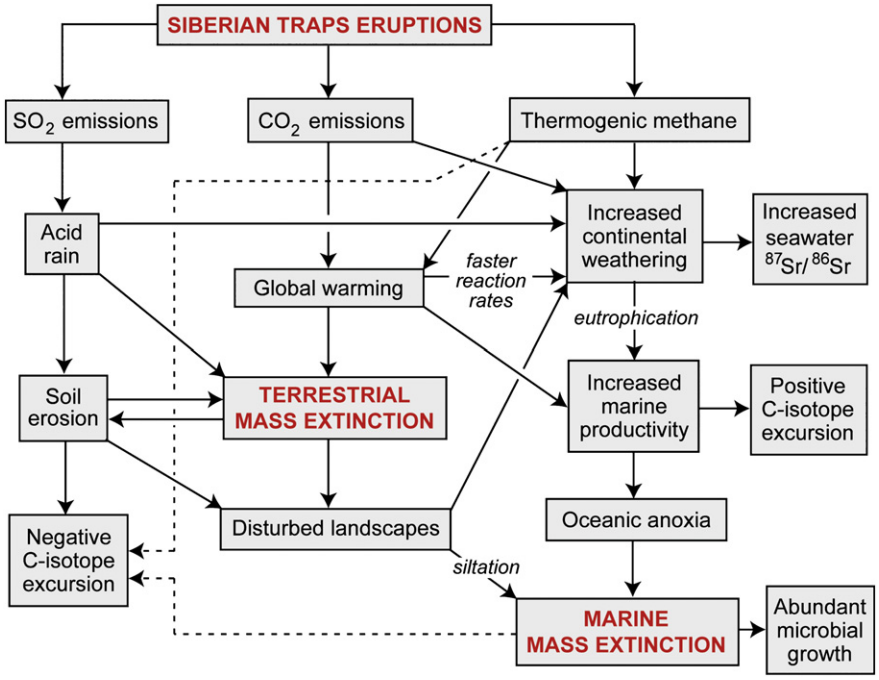


**Fig. 5.** Flowchart model of cause-and-effect relationships during the LPE crisis and Early Triassic recovery intervals. Modified from Wignall (2001); relative to Wignall's version, features that were poorly documented (e.g., glaciation, sea-level fall, gas hydrate dissociation) have been eliminated, and features for which recent evidence has been adduced (e.g., soil erosion, disturbed landscapes) have been added. Also added are additional links among model features, especially representing inferred terrestrial–marine connections (e.g., continental weathering → marine productivity). Dashed lines indicate possible second-order controls on the negative carbonate C-isotope excursion at the LPE (for which eroded soil organic matter is inferred to be the dominant control).

warming (Retallack, 1999; Retallack & Jahren, 2008), as evidenced by O-isotope studies of marine biogenic calcite (Fig. 2; Kearsey et al., 2009; Korte et al., 2005a,b). Higher levels of atmospheric $CO_2$ along with release of volcanic $SO_2$ is likely to have increased the acidity of precipitation (Self et al., 2008; cf. Sparks et al., 1997; Wignall, 2001, 2007), as evidenced by enhanced chemical weathering of paleosols (Retallack, 1999; Sheldon, 2006). These environmental changes are likely to have been a major factor in the destruction of terrestrial ecosystems in the latest Permian (Figs. 4 and 5). At that time, mature gymnosperm-dominated floras were replaced by rapidly growing early successional communities dominated by lycopsids and ferns (Grauvogel & Ash, 2005; Krassilov & Karasev, 2009; Looy et al., 1999, 2001; Wang, 1996), resulting in reduced sequestration of organic matter in terrestrial facies during the so-called Early Triassic "coal gap" (Retallack et al., 1996). An additional cause and/or consequence of changes in terrestrial floras was change in annual precipitation in some regions. In a study of paleosols from the Kazakhstan plate, Thomas et al. (2011-this issue) document a pattern of climatic drying from the Late Permian, when precipitation was a relatively stable ~1100 mm $year^{-1}$, to the Early Triassic, when precipitation fluctuated widely from ~230 to 1000 mm $year^{-1}$. However, other regions may have experienced a shift toward wetter conditions during the Early Triassic (Kozur, 1998; Krassilov & Karasev, 2009).

The destruction of terrestrial ecosystems is likely to have had profound consequences for weathering processes, nutrient fluxes, and marine environmental conditions (Figs. 4 and 5). Widespread loss of vegetative cover is thought to have led to massive erosion in terrestrial areas during the latest Permian, as shown by a shift from fine-grained meandering to conglomeratic braided fluvial facies (López-Gómez et al., 2005; Michaelsen, 2002; Newell et al., 1999; Ward et al., 2000), by transported soil clasts (pedoliths; Retallack, 2005), by increased sedimentation rates in terrestrial successions (Retallack, 1999), and by an abrupt influx of terrigenous siliciclastics to carbonate platforms in China (Tong et al., 2007b), Oman (Weidlich & Bernecker, 2011-this issue), and elsewhere (Algeo & Twitchett, 2010). In addition, the signature of this erosion event has been recognized in the form of soil-derived biomarkers (Sephton et al., 2005; Wang & Visscher, 2007; Xie et al., 2005, 2007) and nutrient-stimulated algal blooms (Afonin et al., 2001; Kozur, 1998). Both features generally appear just below the LPE horizon, suggesting that the influx of eroded soils played a role in the marine biotic crisis (Sephton et al., 2005). However, soil biomarkers have not been documented from the Lower Triassic of marine successions, suggesting that the soil erosion event was brief, and that subsequent increases in marine sedimentation rates were due to bedrock erosion (Fig. 3; Algeo & Twitchett, 2010).

Subaerial erosion rates increased sharply during the latest Permian and remained high for a protracted (~2 Myr-long) interval during the Early Triassic (Fig. 3). The increased flux of eroded material resulted in an average ~7-fold increase in sedimentation rates in shallow-marine systems globally as well as by a shift toward more clay-rich compositions in both carbonate and siliciclastic marine facies (Algeo & Twitchett, 2010). The observation that sedimentation rates increased concurrently with higher clay contents in marine successions is important because it rules out more commonplace interpretations based on sequence stratigraphic, eustatic, and tectonic controls, in which increasing clay content in siliciclastic successions is generally associated with reduced sedimentation rates (e.g., as a function of eustatic rise). Intensification of chemical weathering rates during the Early Triassic was probably a consequence of faster soil reaction rates (due to warmer temperatures; Korte et al., 2005a,b), increased acidity of precipitation (Wignall, 2001, 2007), and the vulnerability of ecologically disturbed landscapes to erosion (Figs. 4 and 5; Looy et al., 1999, 2001). Evidence for enhanced chemical weathering during the Early Triassic is supported by geochemical changes in paleosols (Retallack, 1999; Sheldon, 2006) as well as by shifts toward more radiogenic (continent-derived) compositions in the seawater Sr and Nd isotope records (Korte et al., 2003, 2006; Martin & Macdougall, 1995).

Enhanced sediment fluxes would have had profound, mostly negative consequences for benthic marine biotas (Fig. 1; Algeo & Twitchett, 2010). At the organismal level, elevated turbidity causes a reduction in feeding activity, osmoregulation, growth rate, body size, larval recruitment, development, and survival. Suspension feeders

suffer because of reduced seston quality and the elevated energy costs involved in the removal of inorganic particles, and grazers suffer if sediment influx is great enough to bury and kill off their food source. High inorganic nutrient (N and P) concentrations lead to other harmful effects, including lower rates of skeletal calcification, inhibited fertilization and larval survival, and decreased resistance to borers and disease. Changes in substrate consistency due to high sediment influx may have favored organisms adapted to soft, unstable substrates (e.g., 'paper pectens' such as *Claraia*; Fig. 1B) and reduced ecological tiering in Early Triassic marine ecosystems (Fraiser & Bottjer, 2005). Although the resilience of aquatic organisms to sediment influx is clade- and taxon-specific, experimental and observational studies have shown that flux increases of 5–20× induce severe biotic stress and increases of 20–100× generally result in mortality (Algeo & Twitchett, 2010). The harmful effects of elevated detrital fluxes on Early Triassic marine ecosystems may have been particularly great given that sedimentation rates remained high for several million years during the Early Triassic (Fig. 3).

Elevated sediment fluxes were not the only harmful factor affecting Early Triassic marine ecosystems. Other factors that contributed to marine extinctions and to degradation of marine communities at this time included elevated seawater temperatures, hypercapnia, and benthic hypoxia/anoxia (Figs. 4 and 5; Knoll et al., 2007; Pörtner et al., 2005). O-isotopic data document a ca. −2 to −3‰ shift in low-latitude regions across the LPE horizon, equivalent to a warming of ~8 to 10 °C, assuming no ice-volume effect (Kearsey et al., 2009; Korte et al., 2005a,b). A warming of this magnitude would have had a strongly adverse impact on marine life (Knoll et al., 2007). Upwelling of $CO_2$ from anoxic deep-ocean waters during the LPE may have increased the acidity of surface waters for a transient period, causing elevated mortality among carbonate-secreting organisms (Fraiser & Bottjer, 2007; Knoll et al., 1996, 2007). Euxinia, i.e., a lack of dissolved oxygen along with free $H_2S$ in the water column, developed widely on continent margins and platform settings, as documented by various proxies including biomarkers, pyrite framboid sizes and S-isotopic compositions, and Ce anomalies (Cao et al., 2009; Grice et al., 2005; Kakuwa & Matsumoto, 2006; Nielsen & Shen, 2004; Riccardi et al., 2006; Wignall et al., 2005). However, redox patterns in shallow-marine environments were complex, exhibiting strong spatial and temporal variability (Algeo et al., 2007a,b, 2008; Bond & Wignall, 2010).

Redox changes in shallow-marine environments during the latest Permian and Early Triassic may have been caused either by chemocline upward excursions (Kump et al., 2005; Riccardi et al., 2006) or by upwelling of deep anoxic watermasses (Fig. 4; Algeo et al., 2007a, 2008). Clues to the mechanism responsible for these changes in Permian–Triassic seawater chemistry have been sought in the marine carbonate C-isotopic record, which shows large excursions throughout the Early Triassic (Fig. 2; Horacek et al., 2007a,b; Payne et al., 2004). Despite considerable effort to constrain process on the basis of C-isotopic profiles, it is clear that the C-isotopic fluctuations characteristic of the latest Permian and Early Triassic could have been produced by several mechanisms (Berner, 2002; Payne & Kump, 2007). Indeed, multiple mechanisms may have operated concurrently, perhaps with temporally variable intensities, to yield the patterns observed globally (Corsetti et al., 2005). Whereas additional C-isotope data alone are unlikely to resolve this situation, new insights may be gained through examination of patterns of C-isotopic covariation with other geochemical proxies. For example, negative $\delta^{13}C_{carb}$ excursions in sections of the South China craton have been shown to correlate with increases in $C_{30}$-M/$C_{30}$-HP and 2-MeHI biomarker ratios (Xie et al., 2007) and with increased concentrations of $^{34}S$-depleted pyrite (Algeo et al., 2007a, 2008). The latter study documented at least 8 intervals characterized by $\delta^{13}C_{carb}$-pyrite covariation, providing evidence of multiple episodes of upwelling of $^{13}C$-depleted, sulfidic deepwaters onto shallow carbonate platforms of the Nanpanjiang Basin (Algeo et al., 2007a, 2008).

The global ocean also experienced redox changes during the PTB crisis interval, as inferred from sections in Japan and western Pangea (Algeo et al., 2010, 2011-this issue; Isozaki, 1997; Wignall et al., 2009). Isozaki (1997) hypothesized a >10-Myr-long interval of oceanic "superanoxia" through most or all of the Late Permian and Early Triassic, but recent work has shown that the Late Permian deep-ocean environment was probably suboxic rather than anoxic (Algeo et al., 2010, 2011-this issue; Brennecka et al., submitted for publication; Wignall et al., 2009; ). Changes in oceanic redox conditions in conjunction with the LPE were most pronounced within the oxygen-minimum zone (OMZ) at intermediate water depths, where euxinic conditions developed and large quantities of pyrite framboids formed before sinking to the deep seafloor (Fig. 4; Algeo et al., 2010, 2011-this issue). These findings support the results of modeling studies regarding the non-feasibility of prolonged stagnation of deep-ocean circulation in conjunction with the PTB crisis (Hotinski et al., 2001; Kiehl & Shields, 2005). Rather, expansion of oceanic anoxia primarily within the OMZ points toward the role of heightened marine productivity and organic carbon export from ocean-surface waters (Figs. 4 and 5; Algeo et al., 2010, 2011-this issue; Meyer et al., 2008; Winguth & Maier-Reimer, 2005).

Enhanced marine productivity was a likely consequence of elevated chemical weathering rates and terrestrially sourced nutrient fluxes during the Early Triassic (Algeo & Twitchett, 2010). High-resolution stratigraphic records suggest a possibly tight coupling between changes in weathering rates and changes in marine ecosystems. Bedrock erosion rates (as proxied by marine sedimentation rates) appear to have peaked several times during the Early Triassic, specifically in the early to late Griesbachian, around the Induan–Olenekian boundary, and (more speculatively) in the mid-Spathian (Fig. 3; Algeo, unpubl. data). These times also correspond to maxima in the marine carbonate $\delta^{13}C$ record, episodes of widespread microbial mat growth, and peaks in conodont and ammonoid diversity (Fig. 3). Changes in weathering fluxes may be the key to understanding the relationship between these developments: increased fluxes of nutrients to marine systems would have created eutrophic conditions (favoring stromatolitic microbes over corals and other oligotrophic organisms), stimulated marine productivity and organic carbon burial fluxes (proxied by higher carbonate $\delta^{13}C$ values), and increased energy flows to higher trophic levels (represented by conodont and ammonoid diversity; Fig. 4). These relationships are consistent except for during the LPE, when marine carbonate $\delta^{13}C$ values declined despite increased erosion rates. The key difference is that erosion of soils during the LPE mobilized a huge reservoir of $^{13}C$-depleted soil organic carbon that overwhelmed any trend toward higher carbonate $\delta^{13}C$ values as a function of enhanced marine productivity. The latest Permian shift toward lower $\delta^{13}C$ values may have been reinforced also by emissions of highly $^{12}C$-enriched thermogenic methane during magmatic intrusions into West Siberian coalfields (Fig. 5; Retallack & Jahren, 2008).

The full recovery of marine ecosystems following the PTB crisis was remarkably slow, extending over the ~5 Myr duration of the Early Triassic (Figs. 1 and 2; Bottjer et al., 2008). The delay in recovery may have been due to one or more of the following causes: (1) persistently hostile environmental conditions in the aftermath of the boundary crisis (Hallam, 1991; Isozaki, 1997; Payne et al., 2004), (2) episodic recurrence of environmental perturbations that suppressed marine ecosystem recovery (Algeo et al., 2007a, 2008; Orchard, 2007; Retallack et al., 2011-this issue; Stanley, 2009), or (3) such complete loss of biodiversity that the pace of ecosystem reconstruction was limited by timescales of biotic evolution and ecosystem reintegration (Erwin, 2001, 2007). There seems to be some evidence to support each of these hypotheses, and all of them may have operated in tandem. Episodic environmental stresses seem to be indicated by large swings in the carbonate C-isotope record (Fig. 2; Horacek et al., 2007a,b; Payne et al., 2004), although whether these excursions represent external forcings (e.g., injection of isotopically light C) or

internal ecosystem dynamics (e.g., large fluctuations in rates of marine productivity and organic carbon burial) is unclear (Fig. 5). In their study of Lower Triassic terrestrial successions of the Sydney Basin of southeastern Australia, Retallack et al. (2011-this issue) identify multiple horizons recording C-isotopic excursions and changes in chemical weathering intensity, based on which they infer that recurrent environmental perturbations may have been a key factor in the delayed recovery of marine ecosystems during the Early Triassic. However, further work will be needed to elucidate the rate and pattern of biotic recovery following the PTB crisis and its relationship to external forcings and internal ecosystem dynamics.

## Acknowledgments

Thanks to Matthew Clapham and Paul Wignall for the reviews and to David Bottjer for editorial handling. Research by TJA was supported by the National Science Foundation grants EAR-0618003 and EAR-0745574. This paper is a contribution to IGCP Project 572.

## References

Afonin, S.A., Barinova, S.S., Krassilov, V.A., 2001. A bloom of zygnematalean green algae *Tympanicysta* at the Permian–Triassic boundary. Geodiversitas 23, 481–487.
Algeo, T.J., Twitchett, R.J., 2010. Anomalous Early Triassic sediment fluxes due to elevated weathering rates and their biological consequences. Geology 38, 1023–1026.
Algeo, T.J., Ellwood, B.B., Thoa, N.T.K., Rowe, H., Maynard, J.B., 2007a. The Permian–Triassic boundary at Nhi Tao, Vietnam: evidence for recurrent influx of sulfidic watermasses to a shallow-marine carbonate platform. Palaeogeogr. Palaeoclimatol. Palaeoecol. 252, 304–327.
Algeo, T.J., Hannigan, R., Rowe, H., Brookfield, M., Baud, A., Krystyn, L., Ellwood, B.B., 2007b. Sequencing events across the Permian–Triassic boundary, Guryul Ravine (Kashmir, India). Palaeogeogr. Palaeoclimatol. Palaeoecol. 252, 328–346.
Algeo, T.J., Shen, Y., Zhang, T., Lyons, T.W., Bates, S.M., Rowe, H., Nguyen, T.K.T., 2008. Association of $^{34}$S-depleted pyrite layers with negative carbonate $\delta^{13}$C excursions at the Permian/Triassic boundary: evidence for upwelling of sulfidic deep-ocean watermasses. Geochem. Geophys. Geosyst. 9, 10.
Algeo, T.J., Hinnov, L., Moser, J., Maynard, J.B., Elswick, E., Kuwahara, K., Sano, H., 2010. Changes in productivity and redox conditions in the Panthalassic Ocean during the latest Permian. Geology 38, 187–190.
Algeo, T.J., Henderson, C.M., Tong, J., Feng, Q., Yin, H., Tyson, R.V., in review. Plankton and productivity during the Permian–Triassic boundary crisis: an analysis of organic carbon fluxes. Submitted to Global and Planetary Change.
Algeo, T.J., Kuwahara, K., Sano, H., Bates, S., Lyons, T., Elswick, E., Hinnov, L., Ellwood, B., Moser, J., Maynard, J.B., 2011. Spatial variation in sediment fluxes, redox conditions, and productivity in the Permian–Triassic Panthalassic Ocean. Palaeogeogr. Palaeoclimatol. Palaeoecol. 308, 65–83 (this issue).
Alroy, J., et al., 2008. Phanerozoic trends in the global diversity of marine invertebrates. Science 321, 97–100.
Bambach, R.K., Knoll, A.H., Wang, S.C., 2004. Origination, extinction, and mass depletions of marine diversity. Paleobiology 30, 522–542.
Baud, A., Cirilli, S., Marcoux, J., 1997. Biotic response to mass extinction: the lowermost Triassic microbialites. Facies 36, 238–242.
Baud, A., Richoz, S., Pruss, S., 2007. The lower Triassic anachronistic carbonate facies in space and time. Global Planet. Change 55, 81–89.
Beatty, T.W., Zonneveld, J.-P., Henderson, C.M., 2008. Anomalously diverse Early Triassic ichnofossil assemblages in northwest Pangea: a case for a shallow-marine habitable zone. Geology 36, 771–774.
Beauchamp, B., Baud, A., 2002. Growth and demise of Permian biogenic chert along northwest Pangea: evidence for end-Permian collapse of thermohaline circulation. Palaeogeogr. Palaeoclimatol. Palaeoecol. 184, 37–63.
Becker, L., Poreda, R.J., Hunt, A.G., Bunch, T.E., Rampino, M., 2001. Impact event at the Permian–Triassic boundary: evidence from extraterrestrial noble gases in fullerenes. Science 291, 1530–1533.
Becker, L., Poreda, R.J., Basu, A.R., Pope, K.O., Harrison, T.M., Nicholson, C., Iasky, R., 2004. Bedout: a possible end-Permian impact crater offshore of northwestern Australia. Science 304, 1469–1476.
Benton, M.J., 2003. When Life Nearly Died: The Greatest Mass Extinction of All Time. Thames & Hudson, London. 336 pp.
Benton, M.J., Twitchett, R.J., 2003. How to kill (almost) all life: the end-Permian extinction event. Trends Ecol. Evol. 18, 358–365.
Berner, R.A., 2002. Examination of hypotheses for the Permo–Triassic boundary extinction by carbon cycle modeling. Proc. Nat. Acad. Sci. U.S.A. 99, 4172–4177.
Bond, D.P.G., Wignall, P.B., 2010. Pyrite framboid study of marine Permian–Triassic boundary sections: a complex anoxic event and its relationship to contemporaneous mass extinction. Geol. Soc. Am. Bull. 122, 1265–1279.
Bottjer, D.J., Clapham, M.E., Frasier, M.L., Powers, C.M., 2008. Understanding mechanisms for the end-Permian mass extinction and the protracted Early Triassic aftermath and recovery. GSA Today 18, 4–10.
Brayard, A., Bucher, H., Escarguel, G., Fluteau, F., Bourquin, S., Galfetti, T., 2006. The Early Triassic ammonoid recovery: paleoclimatic significance of diversity gradients. Palaeogeogr. Palaeoclimatol. Palaeoecol. 239, 374–395.
Brayard, A., Escarguel, G., Bucher, H., Monnet, C., Brühwiler, T., Goudemand, N., Galfetti, T., Guex, J., 2009. Good genes and good luck: ammonoid diversity and the end-Permian mass extinction. Science 325, 1118–1121.
Brennecka, G.A., Herrmann, A.D., Algeo, T.J., Anbar, A.D., submitted for publication. Timing and extent of global ocean anoxia at the end-Permian extinction. Science, submitted December 2010.
Brett, C.E., 1998. Sequence stratigraphy, paleoecology, and evolution: biotic clues and responses to sea-level fluctuations. Palaios 13, 241–262.
Campbell, I.H., Czamanske, G.K., Fedorenko, V.A., Hill, R.I., Stepanov, V., 1992. Synchronism of the Siberian Traps and the Permian–Triassic boundary. Science 258, 1760–1763.
Cao, C., Love, G.D., Hays, L.E., Wang, W., Shen, S., Summons, R.E., 2009. Biogeochemical evidence for euxinic oceans and ecological disturbance presaging the end-Permian mass extinction event. Earth Planet. Sci. Lett. 281, 188–201.
Chen, Z.Q., McNamara, K.J., 2006. End-Permian extinction and subsequent recovery of the Ophiuroidea (Echinodermata). Palaeogeogr. Palaeoclimatol. Palaeoecol. 236, 321–344.
Chen, Z.Q., Kaiho, K., George, A.D., 2005a. Early Triassic recovery of brachiopod faunas from the end-Permian mass extinction: a global review. Palaeogeogr. Palaeoclimatol. Palaeoecol. 224, 270–290.
Chen, Z.Q., Kaiho, K., George, A.D., 2005b. Survival strategies of brachiopod faunas from the end-Permian mass extinction. Palaeogeogr. Palaeoclimatol. Palaeoecol. 224, 232–269.
Chen, Z.Q., Kaiho, K., George, A.D., Tong, J.N., 2006. Survival brachiopod faunas of the end-Permian mass extinction from northern Italy and south China. Geol. Mag. 243, 301–327.
Chen, J., Beatty, T.W., Henderson, C.M., Rowe, H., 2009a. Conodont biostratigraphy across the Permian–Triassic boundary at the Dawen section, Great Bank of Guizhou, Guizhou Province, South China: implications for the Late Permian extinction and correlation with Meishan. J. Asian Earth Sci. 36, 442–458.
Chen, Z.Q., Tong, J., Zhang, K., Yang, H., Liao, Z., Song, H., Chen, J., 2009b. Environmental and biotic turnover across Permian–Triassic boundary from shallow carbonate platform in western Zhejiang, South China. Aust. J. Earth Sci. 56, 775–797.
Chen, Z.Q., Tong, J., Liao, Z.T., Chen, J., 2010. Structural changes of marine communities over the Permian–Triassic transition: ecologically assessing the end-Permian mass extinction and its aftermath. Glob. Planet. Change 73, 123–140.
Chen, J., Chen, Z.Q., Tong, J., 2011a. Environmental determinants and ecologic selectivity of benthic faunas from nearshore to bathyal zones in the end-Permian mass extinction: Brachiopod evidence from South China. Palaeogeogr. Palaeoclimatol. Palaeoecol. 308, 84–97 (this issue).
Chen, L., Wang, Y., Xie, S., Kershaw, S., Dong, M., Yang, H., Liu, H., Algeo, T.J., 2011b. Molecular records of microbialites following the end-Permian mass extinction in Chongyang, Hubei Province, South China. Palaeogeogr. Palaeoclimatol. Palaeoecol. 308, 151–159 (this issue).
Clapham, M.E., Bottjer, D.J., 2007. Prolonged Permian–Triassic ecological crisis recorded by molluscan dominance in Late Permian offshore assemblages. Proc. Nat. Acad. Sci. U.S.A. 104, 12,971–12,975.
Clapham, M.E., Bottjer, D.J., Powers, C.M., Bonuso, N., Fraiser, M.L., Marenco, P.J., Dornbos, S.Q., Pruss, S.B., 2006. Assessing phanerozoic marine invertebrate ecological dominance. Palaios 21, 431–441.
Corsetti, F.A., Baud, A., Marenco, P.J., Richoz, S., 2005. Summary of Early Triassic carbon isotope records. C.R. Palevol 4, 405–418.
Erwin, D.H., 1994. The Permo-Triassic extinction. Nature 367, 231–236.
Erwin, D.H., 2001. Lessons from the past: biotic recoveries from mass extinctions. Proc. Nat. Acad. Sci. U.S.A. 98, 5399–5403.
Erwin, D.H., 2007. Increasing returns, ecological feedback and the Early Triassic recovery. Palaeoworld 16, 9–15.
Farley, K.A., Garrison, G., Mukhopadhyay, S., Ward, P., 2005. Absence of extraterrestrial $^{3}$He in Permian–Triassic age sedimentary rocks. Earth Planet. Sci. Lett. 240, 265–275.
Feng, Q., He, W., Gu, S., Meng, Y., Jin, Y., Zhang, F., 2007. Radiolarian evolution during the latest Permian in South China. Global Planet. Change 55, 177–192.
Flügel, E., 2002. Triassic reef patterns. In: Kiessling, W., Flügel, E., Golonka, J. (Eds.), Phanerozoic Reef Patterns: SEPM (Society for Sedimentary Geology) Spec. Publ., 72, pp. 391–463.
Forel, M.-B., Crasquin, S., Brühwiler, T., Goudemand, N., Bucher, H., Baud, A., Randon, C., 2011. Ostracod recovery after Permian–Triassic boundary mass-extinction: The south Tibet record. Palaeogeogr. Palaeoclimatol. Palaeoecol. 308, 160–170 (this issue).
Fraiser, M.L., 2011. Paleoecology of secondary tierers from Western Pangean tropical marine environments during the aftermath of the end-Permian mass extinction. Palaeogeogr. Palaeoclimatol. Palaeoecol. 308, 181–189 (this issue).
Fraiser, M.L., Bottjer, D.J., 2004. The non-actualistic Early Triassic gastropod fauna; a case study of the Lower Triassic Sinbad Limestone Member. Palaios 19, 259–275.
Fraiser, M.L., Bottjer, D.J., 2005. Restructuring in benthic level-bottom shallow marine communities due to prolonged environmental stress following the end-Permian mass extinction. C.R. Palevol 4, 515–523.
Fraiser, M.L., Bottjer, D.J., 2007. Elevated atmospheric $CO_2$ and the delayed biotic recovery from the end-Permian mass extinction. Palaeogeogr. Palaeoclimatol. Palaeoecol. 252, 164–175.
Galfetti, T., Bucher, H., Ovtcharova, M., Schaltegger, U., Brayard, A., Brühwiler, T., Goudemand, N., Weissert, H., Hochuli, P.A., Cordey, F., Guodun, K., 2007. Timing of the Early Triassic carbon cycle perturbations inferred from new U-Pb ages and ammonoid biochronozones. Earth Planet. Sci. Lett. 258, 593–604.

Grauvogel-Stamm, L., Ash, S.R., 2005. Recovery of the Triassic land flora from the end-Permian life crisis. C.R. Palevol 4, 593–608.
Greene, S.E., Bottjer, D.J., Hagdorn, H., Zonneveld, J.-P., 2011. The Mesozoic return of Paleozoic faunal constituents: A decoupling of taxonomic and ecological dominance during the recovery from the end-Permian mass extinction. Palaeogeogr. Palaeoclimatol. Palaeoecol. 308, 224–232 (this issue).
Grice, K., Cao, C., Love, G.D., Böttcher, M.E., Twitchett, R.J., Grosjean, E., Summons, R.E., Turgeon, S.C., Dunning, W., Jin, Y., 2005. Photic zone euxinia during the Permian–Triassic superanoxic event. Science 307, 706–709.
Groves, J.R., Altiner, D., 2005. Survival and recovery of calcareous foraminifera pursuant to the end-Permian mass extinction. C.R. Palevol 4, 419–432.
Hallam, A., 1991. Why was there a delayed radiation after the end-Palaeozoic extinctions? Hist. Biol. 5, 257–262.
Horacek, M., Brandner, R., Abart, R., 2007a. Carbon isotope record of the P/T boundary and the Lower Triassic in the Southern Alps: evidence for rapid changes in storage of organic carbon. Palaeogeogr. Palaeoclimatol. Palaeoecol. 252, 347–354.
Horacek, M., Richoz, S., Brandner, R., Krystyn, L., Spötl, C., 2007b. Evidence for recurrent changes in Lower Triassic oceanic circulation of the Tethys: the $\delta^{13}C$ record from marine sections in Iran. Palaeogeogr. Palaeoclimatol. Palaeoecol. 252, 355–369.
Hotinski, R.M., Bice, K.L., Kump, L.R., Najjar, R.G., Arthur, M.A., 2001. Ocean stagnation and end-Permian anoxia. Geology 29, 7–10.
Isozaki, Y., 1997. Permo-Triassic boundary superanoxia and stratified superocean; records from lost deep sea. Science 276, 235–238.
Isozaki, Y., 2009. Integrated "plume winter" scenario for the double-phased extinction during the Paleozoic–Mesozoic transition: the G-LB and P-TB events from a Panthalassic perspective. J. Asian Earth Sci. 36, 459–480.
Isozaki, Y., Aljinović, D., Kawahata, H., 2011. The Guadalupian (Permian) Kamura event in European Tethys. Palaeogeogr. Palaeoclimatol. Palaeoecol. 308, 12–21 (this issue).
Isozaki, Y., Kawahata, H., Minoshima, K., 2007a. The Capitanian (Permian) Kamura cooling event: the beginning of the Paleozoic–Mesozoic transition. Palaeoworld 16, 16–30.
Isozaki, Y., Kawahata, H., Ota, A., 2007b. A unique carbon isotope record across the Guadalupian–Lopingian (Middle–Upper Permian) boundary in mid-oceanic paleoatoll carbonates: the high-productivity "Kamura event" and its collapse in Panthalassa. Global Planet. Change 55, 21–38.
Jablonski, D., 2001. Lessons from the past: evolutionary impacts of mass extinctions. Proc. Nat. Acad. Sci. U.S.A. 98, 5393–5398.
Jablonski, D., 2002. Survival without recovery after mass extinctions. Proc. Nat. Acad. Sci. U.S.A. 99, 8139–8144.
Jacobsen, N., Twitchett, R.J., Krystyn, L., 2011. Palaeoecological methods for assessing marine ecosystem recovery following the Late Permian mass extinction event. Palaeogeogr. Palaeoclimatol. Palaeoecol. 308, 200–212 (this issue).
Ji, W., Tong, J., Zhou, S., Chen, J., 2011. Lower–Middle Triassic conodont biostratigraphy of the Qingyan section, Guizhou Province, Southwest China. Palaeogeogr. Palaeoclimatol. Palaeoecol. 308, 213–223 (this issue).
Kaiho, K., Kajiwara, Y., Nakano, T., Miura, Y., Chen, Z.Q., Shi, G.R., 2001. End-Permian catastrophe by a bolide impact: evidence of a gigantic release of sulfur from the mantle. Geology 29, 815–818.
Kaim, A., Nützel, A., 2011. Dead bellerophontids walking—The short Mesozoic history of the Bellerophontoidea (Gastropoda). Palaeogeogr. Palaeoclimatol. Palaeoecol. 308, 190–199 (this issue).
Kakuwa, Y., Matsumoto, R., 2006. Cerium negative anomaly just before the Permian and Triassic boundary event: the upward expansion of anoxia in the water column. Palaeogeogr. Palaeoclimatol. Palaeoecol. 229, 335–344.
Kearsey, T., Twitchett, R.J., Price, G.D., Grimes, S.T., 2009. Isotope excursions and palaeotemperature estimates from the Permian/Triassic boundary in the Southern Alps (Italy). Palaeogeogr. Palaeoclimatol. Palaeoecol. 279, 29–40.
Kershaw, S., Zhang, Ting-shan, Lan, Guang-zhi, 1999. A microbialite carbonate crust at the Permian–Triassic boundary in South China, and its palaeoenvironmental significance. Palaeogeogr. Palaeoclimatol. Palaeoecol. 146, 1–18.
Kiehl, J.T., Shields, C.A., 2005. Climate simulation of the latest Permian: implications for mass extinction. Geology 33, 757–760.
Knoll, A.H., Bambach, R.K., Canfield, D.E., Grotzinger, J.P., 1996. Comparative Earth history and Late Permian mass extinction. Science 273, 452–457.
Knoll, A.H., Bambach, R.K., Payne, J.L., Pruss, S., Fischer, W.W., 2007. Paleophysiology and end-Permian mass extinction. Earth Planet. Sci. Lett. 256, 295–313.
Korte, C., Kozur, H.W., 2010. Carbon-isotope stratigraphy across the Permian–Triassic boundary: a review. J. Asian Earth Sci. 39, 215–235.
Korte, C., Kozur, H.W., Bruckschen, P., Veizer, J., 2003. Strontium isotope evolution of Late Permian and Triassic seawater. Geochim. Cosmochim. Acta 67, 47–62.
Korte, C., Kozur, H.W., Veizer, J., 2005a. $\delta^{13}C$ and $\delta^{18}O$ values of Triassic brachiopods and carbonate rocks as proxies for coeval seawater and palaeotemperature. Palaeogeogr. Palaeoclimatol. Palaeoecol. 226, 287–306.
Korte, C., Jasper, T., Kozur, H.W., Veizer, J., 2005b. $\delta^{18}O$ and $\delta^{13}C$ of Permian brachiopods: a record of seawater evolution and continental glaciation. Palaeogeogr. Palaeoclimatol. Palaeoecol. 224, 333–351.
Korte, C., Jasper, T., Kozur, H.W., Veizer, J., 2006. $^{87}Sr/^{86}Sr$ record of Permian seawater. Palaeogeogr. Palaeoclimatol. Palaeoecol. 240, 89–107.
Kozur, H.W., 1998. Some aspects of the Permian–Triassic boundary (PTB) and of the possible causes for the biotic crisis around this boundary. Palaeogeogr. Palaeoclimatol. Palaeoecol. 143, 227–272.
Kozur, H.W., Weems, R.E., 2011. Detailed correlation and age of continental late Changhsingian and earliest Triassic beds: Implications for the role of the Siberian Trap in the Permian–Triassic biotic crisis. Palaeogeogr. Palaeoclimatol. Palaeoecol. 308, 22–40 (this issue).
V.Krassilov, V., E.Karasev, E., 2009. Paleofloristic evidence of climate change near and beyond the Permian–Triassic boundary. Palaeogeogr. Palaeoclimatol. Palaeoecol. 284, 326–336.
Krystyn, L., Richoz, S., Baud, A., Twitchett, R.J., 2003. A unique Permian–Triassic boundary section from the Neotethyan Hawasina Basin, Central Oman Mountains. Palaeogeogr. Palaeoclimatol. Palaeoecol. 191, 329–344.
Kump, L.R., Pavlov, A., Arthur, M.A., 2005. Massive release of hydrogen sulfide to the surface ocean and atmosphere during intervals of oceanic anoxia. Geology 33, 397–400.
Lehrmann, D.J., 1999. Early Triassic calcimicrobial mounds and biostromes of the Nanpanjiang basin, South China. Geology 27, 359–362.
Lehrmann, D.J., Ramezani, J., Bowring, S.A., Martin, M.W., Montgomery, P., Enos, P., Payne, J.L., Orchard, M.J., Wang, H., Wei, J., 2006. Timing of recovery from the end-Permian extinction: geochronologic and biostratigraphic constraints from south China. Geology 34, 1053–1056.
Leighton, L.R., 2000. Environmental distribution of spinose brachiopods from the Devonian of New York: test of the soft-substrate hypothesis. Palaios 15, 184–193.
Looy, C.V., Brugman, W.A., Dilcher, D.L., Visscher, H., 1999. The delayed resurgence of equatorial forests after the Permian–Triassic ecological crisis. Proc. Nat. Acad. Sci. U.S.A. 96, 13,857–13,862.
Looy, C.V., Twitchett, R.J., Dilcher, D.L., van Konijnenburg-van Cittert, J.H.A., Visscher, H., 2001. Life in the end-Permian dead zone. Proc. Nat. Acad. Sci. U.S.A. 98, 7879–7883.
López-Gómez, J., Arche, A., Marzo, M., Durand, M., 2005. Stratigraphical and palaeogeographical significance of the continental sedimentary transition across the Permian–Triassic boundary in Spain. Palaeogeogr. Palaeoclimatol. Palaeoecol. 229, 3–23.
Martin, E.E., Macdougall, J.D., 1995. Sr and Nd isotopes at the Permian/Triassic boundary: a record of climate change. Chem. Geol. 125, 73–99.
McGowan, A.J., 2004. Ammonoid taxonomic and morphologic recovery patterns after the Permian–Triassic. Geology 32, 665–668.
McGowan, A.J., 2005. Ammonoid recovery from the Late Permian mass extinction event. C.R. Palevol 4, 449–462.
Metcalfe, B., Twitchett, R.J., Price-Lloyd, N., 2011. Changes in size and growth rate of 'Lilliput' animals in the earliest Triassic. Palaeogeogr. Palaeoclimatol. Palaeoecol. 308, 171–180 (this issue).
Meyer, K.M., Kump, L.R., Ridgwell, A., 2008. Biogeochemical controls on photic-zone euxinia during the end-Permian mass extinction. Geology 36, 747–750.
Michaelsen, P., 2002. Mass extinction of peat-forming plants and the effect on fluvial styles across the Permian–Triassic boundary, northern Bowen Basin, Australia. Palaeogeogr. Palaeoclimatol. Palaeoecol. 179, 173–188.
Müller, R.D., Goncharov, A., Kritski, A., 2005. Geophysical evaluation of the enigmatic Bedout basement high, offshore northwestern Australia. Earth Planet. Sci. Lett. 237, 264–284.
Mundil, R., Ludwig, K.R., Metcalfe, I., Renne, P.R., 2004. Age and timing of the Permian mass extinctions: U/Pb dating of closed-system zircons. Science 305, 1760–1763.
Mundil, R., Pálfy, J., Renne, P.R., Brack, P., 2010. The Triassic time scale: new constraints and a review of geochronological data. In: Lucas, S.G. (Ed.), The Triassic Timescale: Geol. Soc. London Spec. Publ., 334, pp. 41–60.
Newell, A.J., Tverdokhlebov, V.P., Benton, M.J., 1999. Interplay of tectonics and climate on a transverse fluvial system, Upper Permian, Southern Uralian Foreland Basin, Russia. Sediment. Geol. 127, 11–29.
Nielsen, J.K., Shen, Y., 2004. Evidence for sulfidic deep water during the Late Permian in the East Greenland Basin. Geology 32, 1037–1040.
Orchard, M.J., 2007. Conodont diversity and evolution through the latest Permian and Early Triassic upheavals. Palaeogeogr. Palaeoclimatol. Palaeoecol. 252, 93–117.
Ovtcharova, M., Bucher, H., Schaltegger, U., Galfetti, T., Brayard, A., Guex, J., 2006. New Early to Middle Triassic U-Pb ages from South China: Calibration with ammonoid biochronozones and implications for the timing of the Triassic biotic recovery. Earth Planet. Sci. Lett. 243, 463–475.
Parrish, J.T., 1993. Climate of the supercontinent Pangea. J. Geol. 101, 215–233.
Payne, J.L., 2005. Evolutionary dynamics of gastropod size across the end-Permian extinction and through the Triassic recovery interval. Paleobiology 31, 269–290.
Payne, J.L., Kump, L.R., 2007. Evidence for recurrent Early Triassic massive volcanism from quantitative interpretation of carbon isotope fluctuations. Earth Planet. Sci. Lett. 256, 264–277.
Payne, J., van de Schootbrugge, B., 2007. Life in Triassic oceans: links between benthic and planktonic recovery and radiation. In: Falkowski, P.G., Knoll, A.H. (Eds.), The Evolution of Primary Producers in the Sea. Academic Press, New York, pp. 165–189.
Payne, J.L., Lehrmann, D.J., Wei, J., Orchard, M.J., Schrag, D.P., Knoll, A.H., 2004. Large perturbations of the carbon cycle during recovery from the end-Permian extinction. Science 305, 506–509.
Payne, J.L., Lehrmann, D.J., Wei, J., Knoll, A., 2006. The pattern and timing of biotic recovery from the end-Permian extinction on the Great Bank of Guizhou, Guizhou Province, China. Palaios 21, 63–85.
Pörtner, H.O., Langenbuch, M., Michaelidis, B., 2005. Synergistic effects of temperature extremes, hypoxia, and increases in $CO_2$ on marine animals: from Earth history to global change. J. Geophys. Res. 110, C09S10.
Powers, C.M., Pachut, J.F., 2008. Diversity and distribution of Triassic bryozoans in the aftermath of the end-Permian mass extinction. J. Paleontol. 82, 362–371.
Pruss, S.B., Bottjer, D.J., 2004. Late Early Triassic microbial reefs of the western United States: a description and model for their deposition in the aftermath of the end-Permian mass extinction. Palaeogeogr. Palaeoclimatol. Palaeoecol. 211, 127–137.
Pruss, S.B., Bottjer, D.J., 2005. The reorganization of reef communities following the end-Permian mass extinction. C.R. Palevol 4, 485–500.
Racki, G., Cordey, F., 2000. Radiolarian palaeoecology and radiolarites: is the present the key to the past? Earth Sci. Rev. 52, 83–120.

Reichow, M.K., Pringle, M.S., Al'Mukhamedov, A.I., Allen, M.B., Andreichev, V.L., Buslov, M.M., Davies, C.E., Fedoseev, G.S., Fitton, J.G., Inger, S., Medvedev, A.Y., Mitchell, C., Puchkov, V.N., Safanova, I.Y., Scott, R.A., Saunders, A.D., 2009. The timing and extent of the eruption of the Siberian Traps large igneous province: implications for the end-Permian environmental crisis. Earth Planet. Sci. Lett. 277, 9–20.

Renne, P.R., Zheng, Z.C., Richards, M.A., Black, M.T., Basu, A.R., 1995. Synchrony and causal relations between Permian–Triassic boundary crisis and Siberian flood volcanism. Science 269, 1413–1416.

Retallack, G.J., 1995. Permian–Triassic extinction on land. Science 267, 77–80.

Retallack, G.J., 1999. Postapocalyptic greenhouse paleoclimate revealed by earliest Triassic paleosols in the Sydney Basin, Australia. Geol. Soc. Am. Bull. 111, 52–70.

Retallack, G.J., 2005. Earliest Triassic claystone breccias and soil-erosion crisis. J. Sed. Res. 75, 679–695.

Retallack, G.J., Jahren, A.H., 2008. Methane release from igneous intrusion of coal during Late Permian extinction events. J. Geol. 116, 1–20.

Retallack, G.J., Veevers, J.J., Morante, R., 1996. Global early Triassic coal gap between Permo-Triassic extinction and middle Triassic recovery of swamp floras. Geol. Soc. Am. Bull. 108, 195–207.

Retallack, G.J., Sheldon, N.D., Carr, P.F., Fanning, M., Thompson, C.A., Williams, M.L., Jones, B.G., Hutton, A., 2011. Multiple Early Triassic greenhouse crises impeded recovery from Late Permian mass extinction. Palaeogeogr. Palaeoclimatol. Palaeoecol. 308, 233–251 (this issue).

Riccardi, A., Arthur, M.A., Kump, L.R., 2006. Sulfur isotopic evidence for chemocline upward excursions during the end-Permian mass extinction. Geochim. Cosmochim. Acta 70, 5740–5752.

Rodland, D.L., Bottjer, D.J., 2001. Biotic recovery from the end-Permain mass extinction: behavior of the inarticulate brachiopod *Lingula* as a disaster taxon. Palaios 16, 95–101.

Schubert, J.K., Bottjer, D.J., 1992. Early Triassic stromatolites as post-mass extinction disaster forms. Geology 20, 883–886.

Self, S., Blake, S., Sharma, K., Widdowson, M., Sephton, S., 2008. Sulfur and chlorine in Late Cretaceous Deccan magmas and eruptive gas release. Science 319, 1654–1657.

Sephton, M.A., Looy, C.V., Brinkhuis, H., Wignall, P.B., de Leeuw, J.W., Visscher, H., 2005. Catastrophic soil erosion during the end-Permian biotic crisis. Geology 33, 941–944.

Sepkoski Jr., J.J., 1982. A Compendium of Fossil Marine Families: Milwaukee Public Museum Contributions in Biology and Geology, 51, p. 125.

Sepkoski Jr., J.J., 2002. A Compendium of Fossil Marine Animal Genera: Bull. Am. Paleontol., 363, p. 563.

Sheldon, N.D., 2006. Abrupt chemical weathering increase across the Permian–Triassic boundary. Palaeogeogr. Palaeoclimatol. Palaeoecol. 231, 315–321.

Shen, S.-Z., Henderson, C.M., Bowring, S.A., Cao, C.-Q., Wang, Y., Wang, W., Zhang, H., Zhang, Y.-C., Mu, L., 2010. High-resolution Lopingian (Late Permian) timescale of South China. Geol. J. 45, 122–134.

Song, H., Tong, J., Chen, Z.Q., 2009. Two episodes of foraminiferal extinction near the Permian–Triassic boundary at the Meishan section, South China. Aust. J. Earth Sci. 56, 765–773.

Song, H., Tong, J., Chen, Z.Q., 2011. Evolutionary dynamics of the Permian–Triassic foraminifer size: Evidence for Lilliput effect in the End-Permian mass extinction and its aftermath. Palaeogeogr. Palaeoclimatol. Palaeoecol. 308, 98–110 (this issue).

Sparks, R.S.J., Bursik, M.I., Carey, S.N., Gilbert, J.S., Glaze, L.S., Sigurdsson, H., Woods, A.W., 1997. Volcanic Plumes. John Wiley & Sons. 574 pp.

Stanley, S.M., 2009. Evidence from ammonoids and conodonts for multiple Early Triassic mass extinctions. Proc. Nat. Acad. Sci. U.S.A. 106, 15,256–15,259.

Stanley, S.M., Yang, X., 1994. A double mass extinction at the end of the Paleozoic era. Science 266, 1340–1344.

Thomas, S.G., Tabor, N.J., Yang, W., Myers, T.S., Yang, Y., Wang, D., 2011. Palaeosol stratigraphy across the Permian–Triassic boundary, Bogda Mountains, NW China: Implications for palaeoenvironmental transition through earth's largest mass extinction. Palaeogeogr. Palaeoclimatol. Palaeoecol. 308, 41–64 (this issue).

Tong, J., Zhang, S., Zuo, J., Xiong, X., 2007a. Events during Early Triassic recovery from the end-Permian extinction. Global Planet. Change 55, 66–80.

Tong, J.N., Zuo, J.X., Chen, Z.Q., 2007b. Early Triassic carbon isotope excursions from South China: proxies for devastation and restoration of marine ecosystems following the end-Permian mass extinction. Geol. J. 42, 371–389.

Twitchett, R.J., 1999. Palaeoenvironments and faunal recovery after the end-Permian mass extinction. Palaeogeogr. Palaeoclimatol. Palaeoecol. 154, 27–37.

Twitchett, R.J., 2007. The Lilliput effect in the aftermath of the end-Permian extinction event. Palaeogeogr. Palaeoclimatol. Palaeoecol. 252, 132–144.

Twitchett, R.J., Oji, T., 2005. Early Triassic recovery of echinoderms. C.R. Palevol 4, 531–542.

Twitchett, R.J., Krystyn, L., Baud, A., Wheeley, J.R., Richoz, S., 2004. Rapid marine recovery after the end-Permian mass extinction event in absence of marine anoxia. Geology 32, 805–808.

Wang, Z., 1996. Recovery of vegetation from the terminal Permian mass extinction in North China. Rev. Palaeobot. Palynol. 91, 121–142.

Wang, C.J., Visscher, H., 2007. Abundance anomalies of aromatic biomarkers in the Permian–Triassic boundary section at Meishan, China—evidence of end-Permian terrestrial ecosystem collapse. Palaeogeogr. Palaeoclimatol. Palaeoecol. 252, 291–303.

Ward, P.D., Montgomery, D.R., Smith, R., 2000. Altered river morphology in South Africa related to the Permian–Triassic extinction. Science 289, 1740–1743.

Weidlich, O., Bernecker, M., 2011. Biotic carbonate precipitation inhibited during the Early Triassic at the rim of the Arabian Platform (Oman). Palaeogeogr. Palaeoclimatol. Palaeoecol. 308, 129–150 (this issue).

Wignall, P.B., 2001. Large igneous provinces and mass extinctions. Earth Sci. Rev. 53, 1–33.

Wignall, P.B., 2007. The end-Permian mass extinction—how bad did it get? Geobiology 5, 303–309.

Wignall, P.B., Newton, R., Brookfield, M.E., 2005. Pyrite framboid evidence for oxygen-poor deposition during the Permian–Triassic crisis in Kashmir. Palaeogeogr. Palaeoclimatol. Palaeoecol. 216, 183–188.

Wignall, P.B., Sun, Y., Bond, D.P.G., Izon, G., Newton, R.J., Védrine, S., Widdowson, M., Ali, J.R., Lai, X., Jiang, H., Cope, H., Bottrell, S.H., 2009. Volcanism, mass extinction, and carbon isotope fluctuations in the Middle Permian of China. Science 324, 1179–1182.

Winguth, A.M.E., Maier-Reimer, E., 2005. Causes of marine productivity and oxygen changes associated with the Permian–Triassic boundary: a reevalution with ocean general circulation models. Mar. Geol. 217, 283–304.

Woods, A.D., Bottjer, D.J., Mutti, M., Morrison, J., 1999. Lower Triassic large sea-floor carbonate cements: their origin and a mechanism for the prolonged biotic recovery from the end-Permian mass extinction. Geology 27, 645–648.

Xie, S., Pancost, R.D., Yin, H., Wang, H., Evershed, R.P., 2005. Two episodes of microbial change coupled with Permo/Triassic faunal mass extinction. Nature 434, 494–497.

Xie, S., Pancost, R.D., Huang, J., Wignall, P.B., Yu, J., Tang, X., Chen, L., Huang, X., Lai, X., 2007. Changes in the global carbon cycle occurred as two episodes during the Permian–Triassic crisis. Geology 35, 1083–1086.

Yang, H., Chen, Z.Q., Wang, Y., Tong, J., Song, H., Chen, J., 2011. Composition and structure of microbialite ecosystems following the End-Permian mass extinction in South China. Palaeogeogr. Palaeoclimatol. Palaeoecol. 308, 111–128 (this issue).

Zakharov, Y.D., Popov, A.M., this issue. Recovery of the brachiopod and ammonoid faunas from the Permian–Triassic ecological crisis: new evidence from the Lower Triassic of the former USSR. Palaeogeogr. Palaeoclimatol. Palaeoecol.

Zhang, K., Tong, J., Shi, G.R., Lai, X., Yu, J., He, W., Peng, Y., Jin, Y., 2007. Early Triassic conodont-palynological biostratigraphy of the Meishan D section in Changxing, Zhejiang Province, South China. Palaeogeogr. Palaeoclimatol. Palaeoecol. 252, 4–23.

Zhou, M.-F., Malpas, J., Song, X.-Y., Robinson, P.T., Sun, M., Kennedy, A.K., Lesher, C.M., Keays, R.R., 2002. A temporal link between the Emeishan large igneous province (SW China) and the end-Guadalupian mass extinction. Earth Planet. Sci. Lett. 196, 113–122.